

# The impact of awareness diffusion on the spread of COVID-19 based on a two-layer SEIR/V-UA epidemic model

Xueke Zhao | Qingming Zhou | Anjing Wang | Fenping Zhu | Zeyang Meng | Chao Zuo 

School of Management Engineering and E-commerce, Zhejiang Gongshang University, Hangzhou, China

## Correspondence

Chao Zuo, School of Management Engineering and E-commerce, Zhejiang Gongshang University, 310018 Hangzhou, China.  
Email: [chaozuo1982@gmail.com](mailto:chaozuo1982@gmail.com)

## Funding information

General Research Project of Zhejiang Provincial Department of Education, Grant/Award Number: Y 202045064

## Abstract

In this paper, we propose a new susceptible–vaccinated–exposed–infected–recovered with unaware–aware (SEIR/V-UA) model to study the mutual effect between the epidemic spreading and information diffusion. We investigate the dynamic processes of the model with a Kinetic equation and derive the expression for epidemic stability by the eigenvalues of the Jacobian matrix. Then, we validate the model by the Monte Carlo method and numerical simulation on a two-layer scale-free network. With the outbreak of COVID-19, the spread of the epidemic in China prompted drastic measures for transmission containment. We examine the effects of these interventions based on modeling of the information-epidemic and the data of the COVID-19 epidemic case. The results further demonstrate that the epidemic spread can be affected by the effective transmission rate of awareness.

## KEYWORDS

awareness diffusion, epidemic spreading, multiplex networks, SEIR/V-UA model

## 1 | INTRODUCTION

Nowadays, the novel coronavirus disease (COVID-19) as a major health hazard is spreading around the world and has attracted extremely wide public attention.<sup>1–3</sup> There have been many mathematical models proposed to describe the spread of the pandemic. Jia et al.<sup>4</sup> proposed an infectious disease dynamic extended susceptible–infected–recovered (SIR) model to describe the spread of COVID-19 and used time-series data of COVID-19 to estimate the epidemic trend and the basic reproductive number. Cooper et al.<sup>5</sup> developed a SIR model that provided a theoretical framework to investigate the spread of the COVID-19, and used diverse significant parameters to compare the impact of control measures and policies various communities have taken. Liu et al.<sup>6</sup> proposed a susceptible–asymptomatic–infected–recovered (SAIR) model on the social networks to describe the spread of COVID-19 and used the epidemic data to explain why the number of the infected rose in the early stage of the outbreak in Wuhan. Tang et al.<sup>7</sup> studied a deterministic susceptible–exposed–infected–removed (SEIR) compartmental model

to describe the spread of COVID-19 and used the data of the COVID-19 epidemic case to estimate the basic reproduction number. Carcione et al.<sup>8</sup> implemented an SEIR model to calculate the number of infected cases and casualties of the epidemic. Fang et al.<sup>9</sup> studied the parameterized SEIR model to simulate the spread dynamics of the COVID-19 outbreak and conducted a sensitivity analysis to assess the impact of different control measures.

Some researchers further investigated the interaction between epidemic spreading and awareness diffusion, where epidemic spreading in one layer was affected by information propagation taking place in another layer based on the framework of the multiplex networks. Gao et al.<sup>10</sup> combined the spread of information and diseases to propose an unaware–aware–unaware with susceptible–infected–susceptible (UAU-SIS) model and presented a comprehensive analysis to demonstrate a probabilistic description of intra-layer and interlayer dynamical processes by microscopic Markov chain approach (MMCA). Ariful Kabi et al.<sup>11</sup> established a two-layer susceptible–vaccinated–infected–recovered with unaware–aware (SIR/V-UA) epidemic model to study the effect of information spreading in the spatial structure of the

vaccination game on epidemic dynamics. Wang et al.<sup>12</sup> considered an unaware-aware-unaware with susceptible-infected-recovered (UAU-SIR) model to investigate the multiple influences between awareness diffusion and epidemic propagation, and used the MMAC method to demonstrate that epidemic threshold was correlated with the awareness diffusion as well as the topology of epidemic networks. Existing studies indicate that outbreak of an epidemic through a physical contact network can trigger the spreading of information awareness through other different channels, such as online social networks and mass media, which will, in turn, affect epidemic spreading.<sup>13-15</sup>

Considering that the COVID-19 epidemic contains the characteristics of the incubation period, a well-mixed SEIR model can be applied to describe the dynamics of the epidemic process based on the epidemiological characteristics of individuals and clinical progression of COVID-19,<sup>16-19</sup> and the information awareness has a great influence on preventing disease and alerting people toward taking preventative measures against diseases. Therefore, we introduce a coupled model of “SEIR/V-UA” to study the interplay between the COVID-19 epidemic spreading and the diffusion of awareness in multiplex networks.

This paper is organized as follows: In Section 2, we introduce the model, describe the dynamical process evolution, and derive the expression for epidemic stability. In Section 3, we analyze the rationality of the model by the COVID-19 epidemic case. Finally, conclusions and discussions are presented in Section 4.

## 2 | THE COUPLED EPIDEMIC-INFORMATION MODEL

In this study, we introduce the SEIR/V-UA model into a coupled network, which includes two layers, one is a physical layer representing the epidemic spreading with the coefficient of infection rate  $\beta$ , the coefficient of migration rate of latency  $\gamma$ , the rate of recovery  $\mu$ , the coefficient of vaccinated rate  $p$ , the other is the information layer where the diffusion of the awareness evolves with a diffusion rate  $\alpha$ . Moreover, there is a one-to-one correspondence between the nodes of networks in the upper and lower layer, which means that the same node sets will be participated in epidemic spreading and information diffusion in the model, as shown in Figure 1. We will analyze several coupling relations next in our paper.

As the possible changes of state of the nodes and their probabilities at every time step can be represented by dynamic transition diagram, we can get the differential equations<sup>20-22</sup> which describes the dynamical process by using a dynamic transition diagram, as shown in Figure 2.

We separate the  $N$  individuals into five classes in the epidemic layer. At time  $t$ , each individuality  $i$  can be one of the five statuses: Susceptible (S), exposed (E), infected (I), recovered (R), and vaccinated (V). There are two possible states for each individual in the information layer: Unaware (U) or aware (A). When an individual accepts the information of the epidemic from social networks and then transforms the status from unaware to aware in the information layer, these individuals will have a certain probability of being vaccinated.

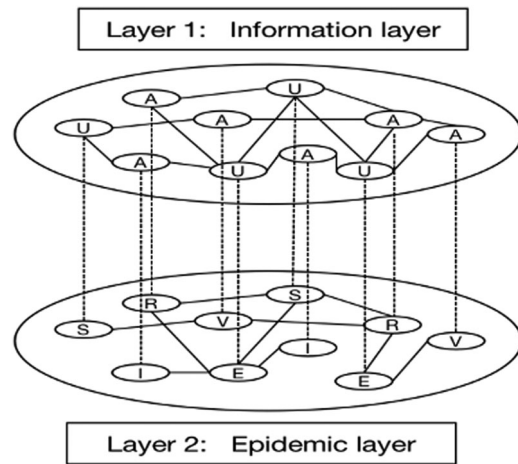


**FIGURE 1** Instruction of the coupled I-E model. Information is diffusing on the upper layer, and the individuals have two possible states: Unaware (U) or aware (A). The epidemic is propagating on the lower layer, where the individuals have five possible states: Susceptible (S), exposed (E), infected (I), recovered (R), and vaccinated (V)

We summarize the definitions of key parameters of the dynamic equation in Table 1.

As shown in Figure 2, equations for the nodes change of each warehouse can be established as the following system:

$$\begin{cases} \frac{dS}{dt} = -\beta \frac{S}{N} I - p \frac{S}{N} A \\ \frac{dE}{dt} = \beta \frac{S}{N} I - \gamma E \\ \frac{dI}{dt} = \gamma E - \mu I \\ \frac{dR}{dt} = \mu I \\ \frac{dV}{dt} = \mu I + p \frac{S}{N} A \\ \frac{dA}{dt} = \alpha \frac{U}{N} A + \gamma E - \mu I \\ \frac{dU}{dt} = -\alpha \frac{U}{N} A - \gamma E + \mu I. \end{cases} \quad (2.1)$$

### 2.1 | Equilibrium analysis

There are three disease-free equilibrium in the following system (2.1):

- (i) The disease-free equilibrium  $E_1 = (N \ 0 \ 0 \ 0 \ 0 \ N)$ .

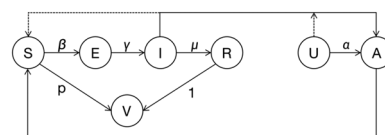


**FIGURE 2** Dynamics of the epidemic based on the susceptible-vaccinated-exposed-infected-recovered model and information propagating unaware-aware model

**TABLE 1** The definitions of key parameters

Parameter	Description
$\alpha$	Probability of becoming aware
$\beta$	The coefficient of infection rate
$\gamma$	The coefficient of migration rate of latency
$\mu$	Probability of recovery
$p$	The coefficient of vaccinated rate

- (ii) The endemic equilibrium  $E_2 = (N \frac{\mu}{\beta} - N \frac{\mu p}{\beta \gamma}, -N \frac{\mu p}{\beta \gamma}, N \frac{\beta \gamma - \gamma p + \mu p}{\beta \gamma}, 0, N)$ .
- (iii) The disease-free equilibrium  $E_3 = (0, 0, 0, N, 0, N)$ .

The Jacobian matrix of the system (2.1) is:

$$J = \begin{pmatrix} -\frac{I\beta}{N} - \frac{AP}{N} & 0 & -\frac{S\beta}{N} & 0 & -\frac{SP}{N} & 0 \\ \frac{I\beta}{N} & -\gamma & \frac{S\beta}{N} & 0 & 0 & 0 \\ 0 & \gamma & -\mu & 0 & 0 & 0 \\ \frac{Ap}{N} & 0 & \mu & 0 & \frac{Sp}{N} & 0 \\ 0 & \gamma & -\mu & 0 & \frac{U\alpha}{N} & \frac{A\alpha}{N} \\ 0 & -\gamma & \mu & 0 & -\frac{U\alpha}{N} & -\frac{A\alpha}{N} \end{pmatrix} \quad (2.2)$$

The Jacobian of the system (2.1) at  $E_1$  is:

$$J(E_1) = \begin{pmatrix} 0 & 0 & \beta & 0 & -p & 0 \\ 0 & -\gamma & \beta & 0 & 0 & 0 \\ 0 & \gamma & -\mu & 0 & 0 & 0 \\ 0 & 0 & \mu & 0 & p & 0 \\ 0 & \gamma & -\mu & 0 & \alpha & 0 \\ 0 & -\gamma & \mu & 0 & -\alpha & 0 \end{pmatrix} \quad (2.3)$$

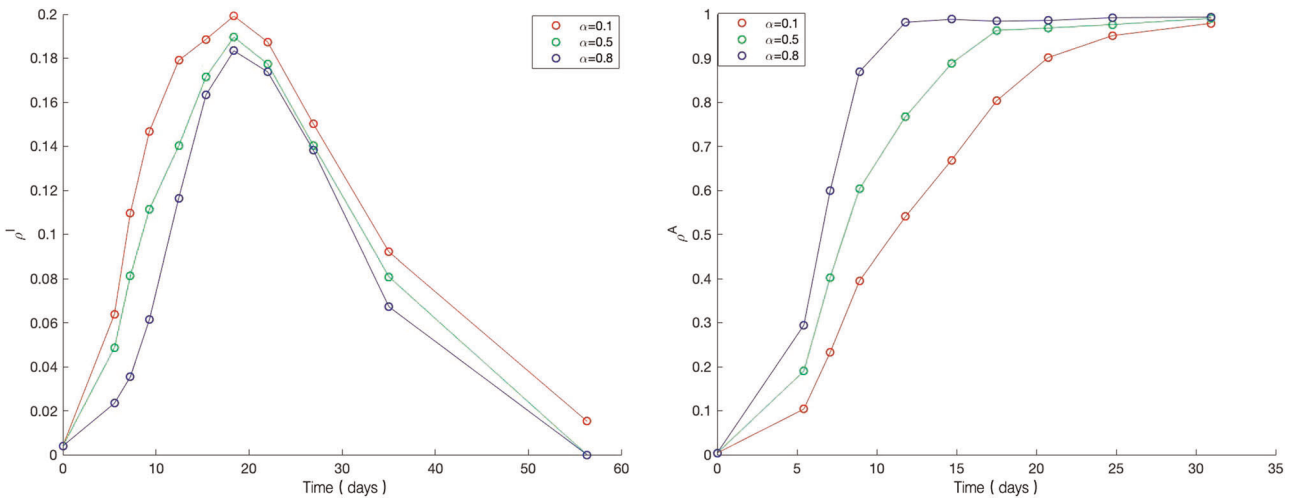


**FIGURE 3**  $\rho^I$  and  $\rho^A$  as functions for different values of  $\alpha$ . The values of other fixed parameters are  $\beta = .3, \gamma = 0.15, \mu = 0.4, p = .6$ . Epidemic layer is a Barabási–Albert network with 5000 nodes (average degree  $\langle k \rangle = 4$ ), the information layer is the same network

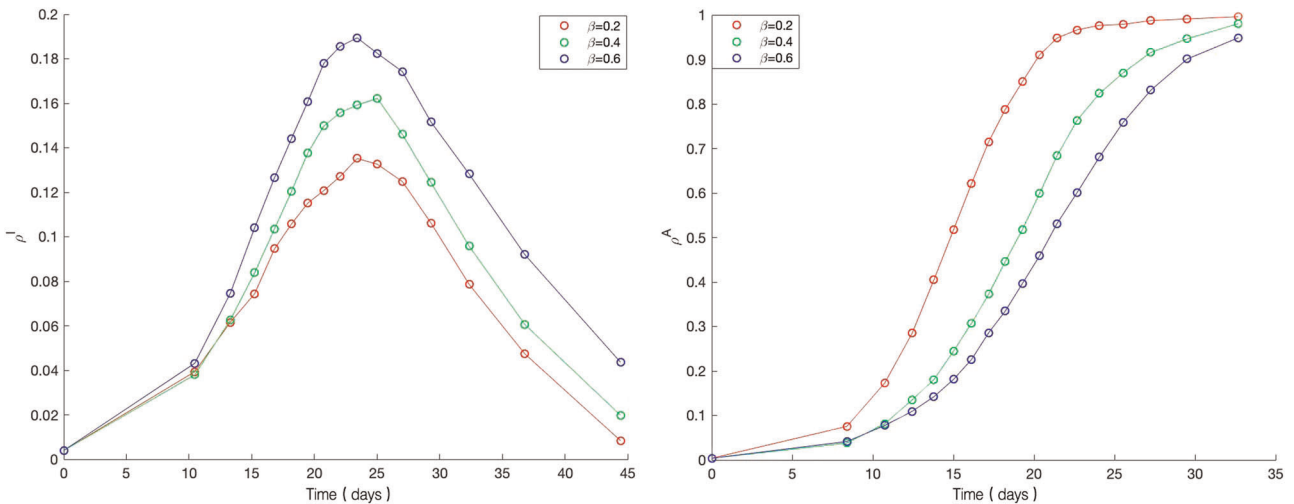


**FIGURE 4**  $\rho^I$  and  $\rho^A$  as functions for different values of  $\beta$ . The values of other fixed parameters are  $\alpha = .3, \gamma = 0.15, \mu = 0.4,$  and  $p = .6$ . Epidemic layer is a Barabási–Albert network with 5000 nodes (average degree  $\langle k \rangle = 4$ ), the information layer is the same network

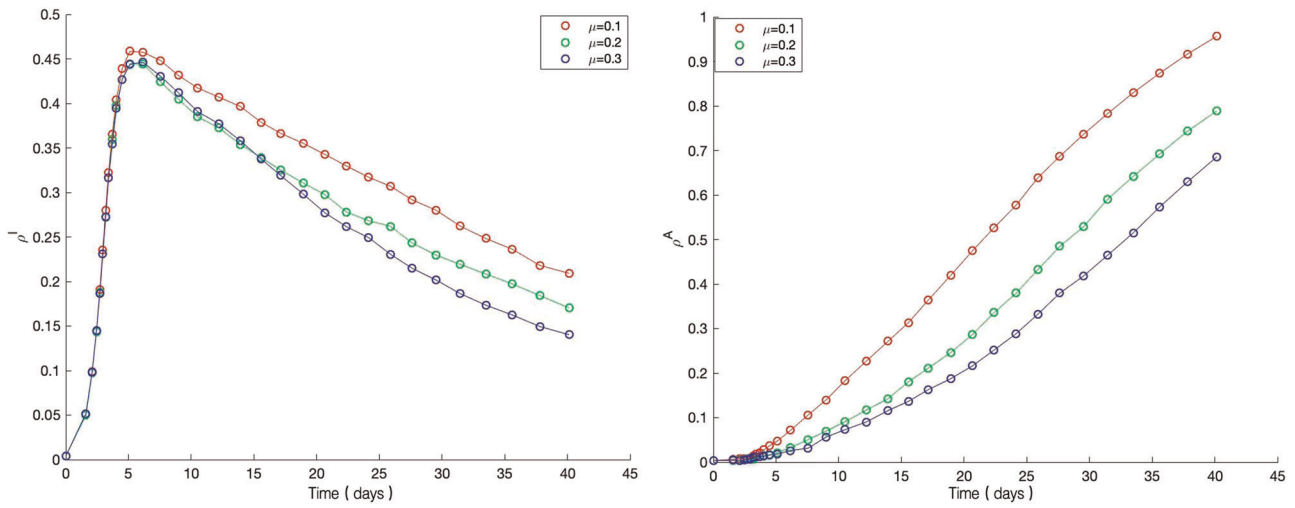


**FIGURE 5**  $\rho^I$  and  $\rho^A$  as functions for different values of  $\mu$ . The values of other fixed parameters are  $\alpha = .3, \beta = .3, \gamma = 0.15$ , and  $p = .6$ . Epidemic layer is a Barabási–Albert network with 5000 nodes (average degree  $\langle k \rangle = 4$ ), the information layers are the same network

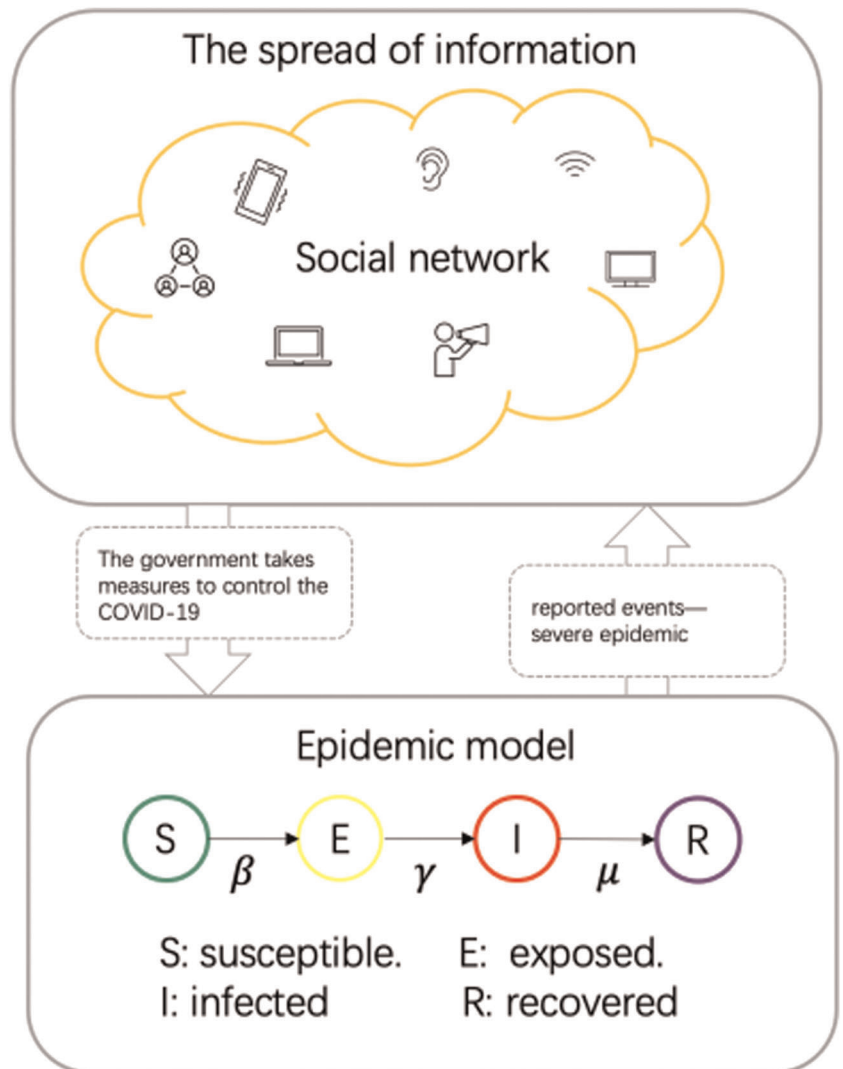


**FIGURE 6** The government takes measures based on information to control the spread of COVID-19

**TABLE 2** Different government control measures and corresponding  $\beta$  values

No.	Date	Government measures	$\beta$	References
1	December 29, 2019–January 22, 2020	(1) Early detection of the COVID-19 (2) Preliminary control	.64	[9] [30]
2	January 23–29, 2020	(1) Public health level 1 response of 31 provinces (2) Strict exit screening (3) Medical support from other regions of China (4) Cancellation of mass gatherings (5) Methodological improvement on the diagnosis and treatment strategy	.46	[9] [30]
3	January 30–February 11, 2020	(1) Public health level 1 response of 31 provinces (2) Strict exit screening (3) Domestic and international medical support (4) The larger scale of cancellation of mass gatherings (5) Further methodological improvement on the diagnosis and treatment strategy (6) Spontaneous household quarantine by citizens (7) Two newly built hospitals' put into use (8) A clinical trial of perspective medicines	.21	[9] [30]
4	February 12–20, 2020	(1) Public health level 1 response of 31 provinces (2) Strict exit screening (3) Further medical support from home and abroad (4) Massive online teaching in a postponed semester (5) Orderly resumption of back to work (6) Addition of new diagnosis method—clinically diagnosis in Hubei province (7) Interagency mechanism (8) Further exploration of effective therapeutic strategy	.09	[9] [30]

Note: The data of COVID-19 in the study were mainly obtained from the National Health Commission of the People's Republic of China, Chinese Center for Disease Control and Prevention, World Health Organization, and various websites of Chinese government agencies, official media, as well as some previous studies as of February 29, 2020.

**TABLE 3** The rate of key parameters

Parameter	Rate	References
$\gamma$	1/7	[9]
$\mu$	1/17.8	[9]

The eigenvalues of this matrix are:

$$e_1 = \left( 0 \ 0 \ 0 \ \alpha - \frac{\gamma}{2} - \frac{\mu}{2} - \frac{(\gamma^2 - 2\gamma\mu + 4\beta\gamma + \mu^2)^{\frac{1}{2}}}{2} \frac{(\gamma^2 - 2\gamma\mu + 4\beta\gamma + \mu^2)^{\frac{1}{2}}}{2} - \frac{\mu}{2} - \frac{\gamma}{2} \right),$$

where  $e_1$  is eigenvalues of the above Jacobian matrix at the point  $E_1$ . It is obvious that  $J(E_1)$  has a positive root. Therefore, the disease-free equilibrium  $E_1$  is an unstable saddle point.<sup>23,24</sup>

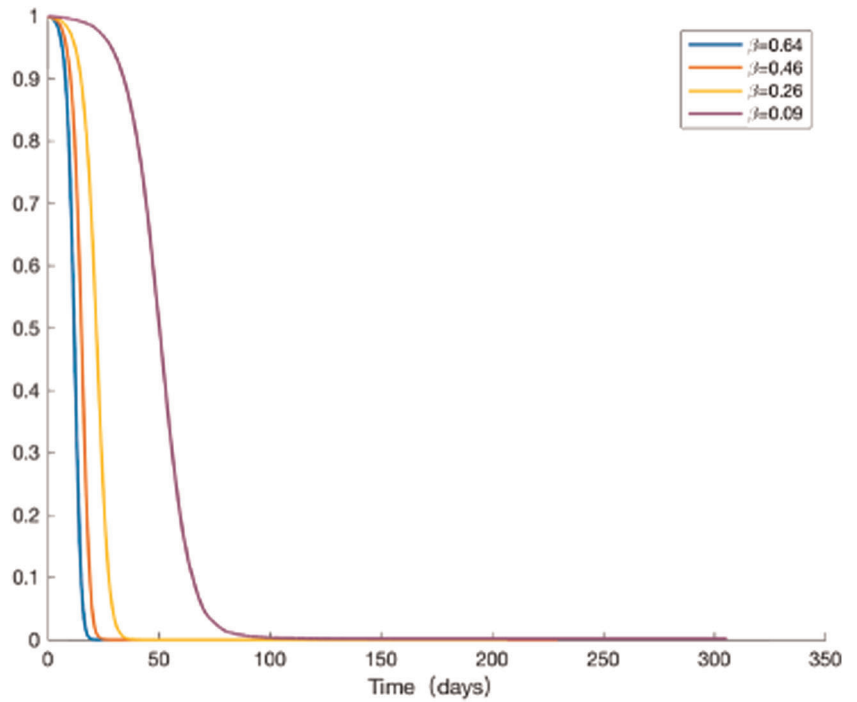
The Jacobian of the system (2.1) at  $E_2$  is:

$$J(E_2) = \begin{pmatrix} 0 & 0 & -\mu & 0 & -\frac{\mu p}{\beta} & 0 \\ -p & -\gamma & \mu & 0 & 0 & 0 \\ 0 & \gamma & -\mu & 0 & 0 & 0 \\ p & 0 & \mu & 0 & \frac{\mu p}{\beta} & 0 \\ 0 & \gamma & -\mu & 0 & 0 & \alpha \\ 0 & -\gamma & \mu & 0 & 0 & -\alpha \end{pmatrix}. \tag{2.4}$$

It is obvious that negative numbers  $\aleph_1 = 0$ , and  $\aleph_2 = 0$  are eigenvalues of  $J(E_2)$ , thus, we only need to consider the roots of  $B_4 \aleph^4 + B_3 \aleph^3 + B_2 \aleph^2 + B_1 \aleph + B_0 = 0$ , where

$$B_4 = \beta > 0,$$

**FIGURE 7** S value simulation curve of the susceptible population



$$B_3 = \gamma\beta + \alpha\beta + \mu\beta > 0,$$

$$B_2 = \alpha\beta\gamma + \alpha\beta\mu + p^2\gamma\mu > 0,$$

$$B_1 = p^2\mu^2\gamma - p\gamma\mu\beta < 0, (\alpha = .5, \beta = .3, \gamma = .15, \mu = 0.4, p = .6),$$

$$B_0 = p^2\gamma\mu^2 - p\alpha\beta\gamma\mu < 0, (\alpha = .5, \beta = .3, \gamma = .15, \mu = .4, p = .6).$$

By a direct calculation, we have that  $B_1 < 0$  and  $B_0 < 0$ . Then by the theorem of Routh–Hurwitz,<sup>25,26</sup> it follows that the epidemic equilibrium  $E_2$  is an unstable saddle point.

The Jacobian of the system (2.1) at  $E_3$  is:

$$J(E_3) = \begin{pmatrix} -p & 0 & 0 & 0 & 0 & 0 \\ 0 & -\gamma & 0 & 0 & 0 & 0 \\ 0 & \gamma & -\mu & 0 & 0 & 0 \\ p & 0 & \mu & 0 & 0 & 0 \\ 0 & \gamma & -\mu & 0 & 0 & \alpha \\ 0 & -\gamma & \mu & 0 & 0 & -\alpha \end{pmatrix}. \tag{2.5}$$

The eigenvalues of this matrix are:

$$e_3 = (0, -\alpha - \gamma - \mu - p),$$

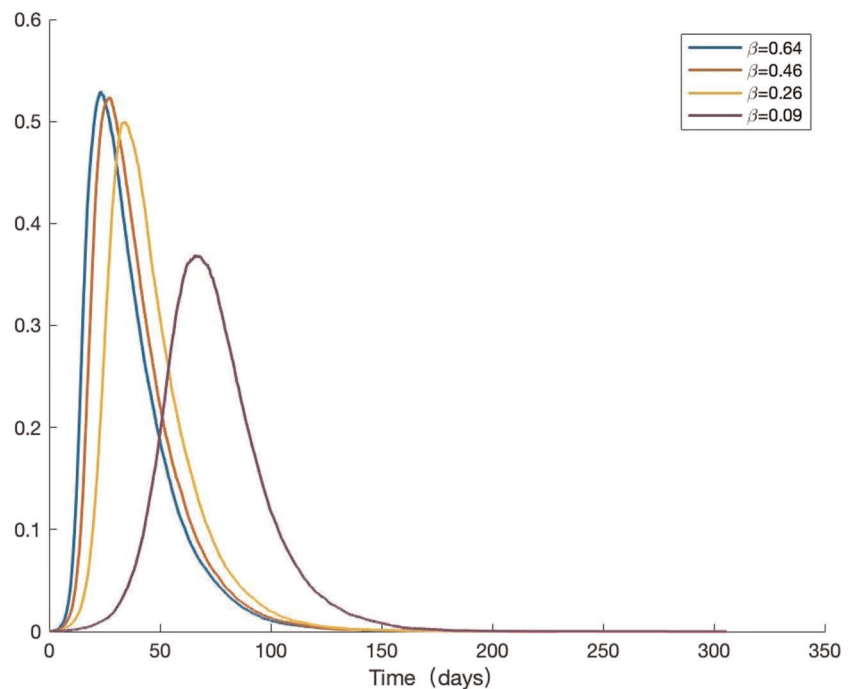


**FIGURE 8** I value simulation curve of the susceptible population

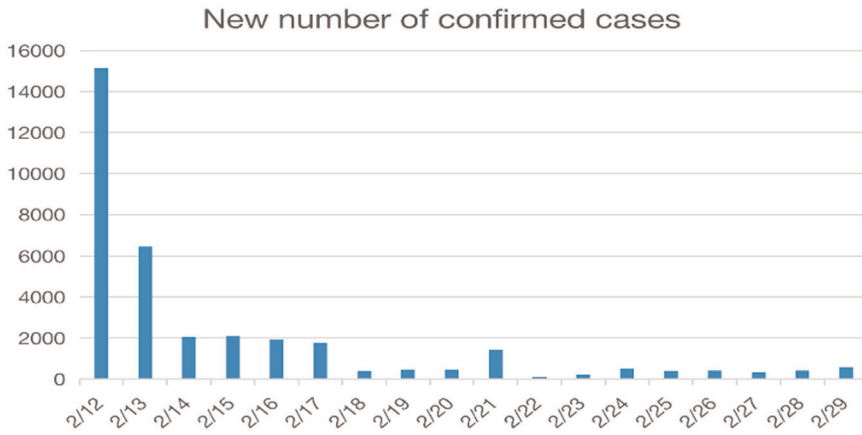


**FIGURE 9** Daily number of new confirmed cases in China

where  $e_3$  is eigenvalues of the above Jacobian matrix at the point  $E_3$ . It is obvious that  $E_3$  has six negative roots. Therefore, the disease-free equilibrium  $E_3$  is asymptotically stable.

## 2.2 | Numerical simulations

We perform extensive Monte Carlo numerical simulations<sup>27,28</sup> for the model by running 1000 times and obtain the  $\rho^A$  and  $\rho^I$ . As shown in Figure 3, we consider the upper layer and lower layer as both scale-free networks with the same average degree  $\langle k \rangle = 4$ . Then we draw the density of infected individuals with a different information transmission rate  $\alpha$  on coupled networks. At the beginning of the outbreak, epidemic spreading and awareness propagation are synchronized and an individual at the epidemic layer is randomly selected as the source of infection. Once an individual in the epidemic layer is infected, the corresponding individual in the information layer will become self-aware and take some protective measures to avoid being infected. Therefore, the probability that an

individual with self-awareness is infected by others will be reduced to some extent.

Then, as awareness rate  $\alpha$  increases, the fraction of infected individuals shows a decreasing tendency from an overall perspective in Figure 3. The phenomenon demonstrates that the rate of awareness individuals in the population will affect the prevalence of epidemic, and it once again shows that awareness plays an important role in the process of epidemic spreading.

And then, as shown in Figure 4, we can observe that the infectious diseases rate  $\beta$  has a greater impact on the prevalence of awareness, and the greater infectious diseases rate  $\beta$  will lead to the higher prevalence of awareness.

Finally, the parameter  $\mu$  has a minimal influence on the density of the number of individuals infected, as shown in Figure 5. On the first layer, the decline of the parameter  $\mu$  indicates that infected individuals are less likely to forget information about the epidemic, causing no apparent influence on the density of disease.

Therefore, in the matter of the value of  $\alpha$ , it is a very effective way to control the epidemic spread by improving the transmission

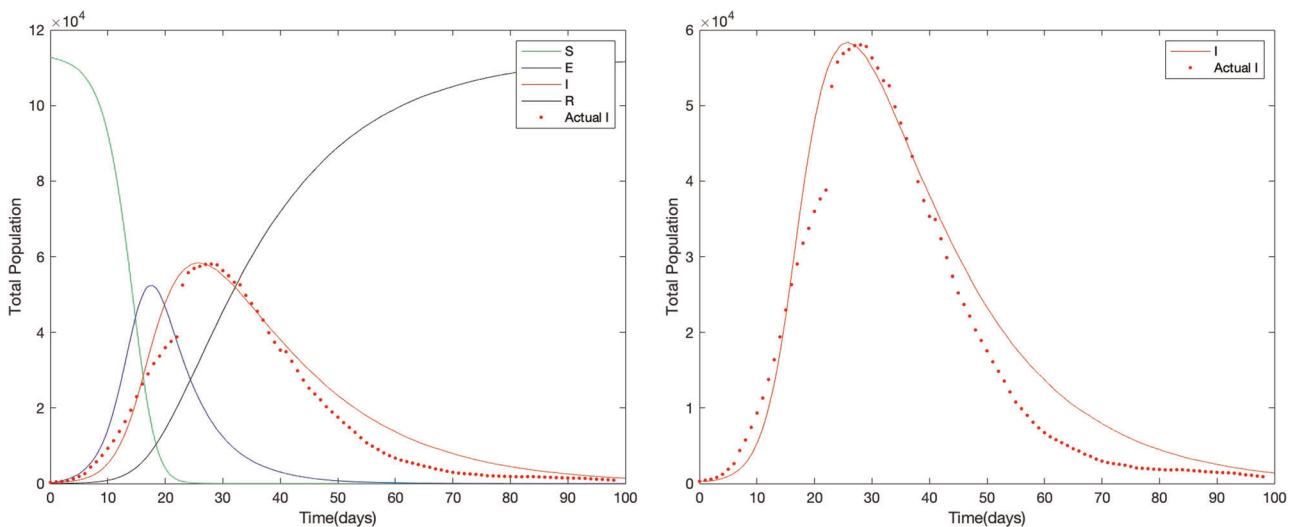


**FIGURE 10** Data fitting of the infected population

rate of information awareness because the individuals who are aware of the epidemic can take effective protection measures.

### 3 | COVID-19 EPIDEMIC ANALYSIS

With the outbreak of the COVID-19, individuals interact with each other through their social relationships to get information about the epidemic (e.g., friendships on Facebook and follower relationships on Twitter).<sup>29</sup> In such a structured host population (i.e., represented by a social network), when the awareness about COVID-19 can spread from person to person as shown in Figure 6, they will take effective measures to protect themselves.

The spread of COVID-19 in China prompted four stages of strict measures for transmission containment. We examine the effects of these interventions based on modeling of the unfolding epidemic and obtain the corresponding rate of key parameters as shown in Tables 2 and 3.

Data fitting is the process of fitting models to data and analyzing the accuracy of the curve, which is performed by Matlab in this study. The  $S$  value curve of the susceptible population and the  $I$  value curve of the infected population can be simulated as shown in Figures 7 and 8. It's clear that the greater the impact of government control policies, the smaller the value of  $\beta$ , the slower the slope of the decline of  $S$  value, and the lower the distribution of the  $I$  value. The data in Figure 9 shows many of the newly confirmed cases on February 12, due to the adoption of new diagnostic methods. Subsequently, the number of newly confirmed cases per day drop rapidly. Figure 10 shows the data fitting curve of the number of infected individuals, indicating that with the strengthening of prevention and control measures, the number of people infected is gradually decreasing.

### 4 | CONCLUSION

In this paper, we propose a SEIR/V-UA model to describe the interplay between epidemic spreading in physical networks and awareness diffusion in information networks.

Then, we conduct theoretical analysis and describe the dynamic process of the coupled network in the form of a Kinetic equation. The expression for epidemic stability is also derived by the eigenvalues of the Jacobian matrix, and all the theoretical calculations are in good agreement with extensive simulation. Therefore, the Kinetic equation plays an important role in analyzing the process of epidemic spreading on a two-layer network.

We research the effect of the three parameters  $\alpha$ ,  $\beta$ , and  $\mu$  on the dynamic propagation process. The parameter  $\alpha$  stands for the rate of diffusion of information about the epidemic, whereas the parameters  $\beta$  and  $\mu$  represent the Infection and recovery rates. The simulation results show that information can affect behavior changes and further affect the dynamic propagation process of the epidemic layer. The parameter  $\alpha$  affects not only the spread of the epidemic but also the diffusion of information on the other layer. The parameter  $\beta$  can

also affect the information layer. However, the parameter  $\mu$  has little influence on the density of the infected individuals, but it can influence the information propagation. This phenomenon indicates that to control the spread of infectious diseases, it is necessary to strengthen self-protection, improve individual immunity and expand information dissemination.

We examine the effects of drastic measures prompted by the Chinese government. Through simulation and data fitting, the model shows the existing peaks and has sufficient goodness of fit. The declines in the dynamic trend of the infected individuals highlight the effectiveness of the four-phase stringent measures the Chinese government has taken.

#### ACKNOWLEDGMENT

This study is supported by the General Research Project of the Zhejiang Provincial Department of Education (Grant No. Y202045064).

#### CONFLICT OF INTERESTS

The authors declare that there are no conflict of interests.

#### AUTHOR CONTRIBUTIONS

Chao Zuo, Xueke Zhao, and Qingming Zhou contributed to model building, data analysis, and writing the paper. Anjing Wang, Fenping Zhu, and Zeyang Meng contributed to data collection and editing the paper.

#### PEER REVIEW

The peer review history for this article is available at <https://publons.com/publon/10.1002/jmv.26945>

#### DATA AVAILABILITY STATEMENT

The data that support the findings of this study are openly available in the National Health Commission of the People's Republic of China at <http://www.nhc.gov.cn/> and References [9] and [30].

#### ORCID

Chao Zuo  <http://orcid.org/0000-0002-5177-5813>

#### REFERENCES

1. Bedford J, Enria D, Giesecke J, et al. COVID-19: towards controlling of a pandemic. *Lancet*. 2020;395(10229):1015-1018.
2. Rothan HA, Byrareddy SN. The epidemiology and pathogenesis of coronavirus disease (COVID-19) outbreak. *J Autoimmun*. 2020;109:102433.
3. Shereen MA, Khan S, Kazmi A, Bashir N, Siddique R. COVID-19 infection: origin, transmission, and characteristics of human coronaviruses. *J Adv Res*. 2020;24:91-98.
4. Wangping J, Ke H, Yang S, et al. Extended SIR prediction of the epidemics trend of COVID-19 in Italy and compared with Hunan, China. *Front Med*. 2020;7:169.
5. Cooper I, Mondal A, Antonopoulos CG. A SIR model assumption for the spread of COVID-19 in different communities. *Chaos, Solitons Fractals*. 2020;139:110057.



6. Liu C, Wu X, Niu R, Wu X, Fan R. A new SAIR model on complex networks for analysing the 2019 novel coronavirus (COVID-19). *Nonlinear Dyn.* 2020;101(3):1777-1787.
7. Tang B, Wang X, Li Q, et al. Estimation of the transmission risk of the 2019-nCoV and its implication for public health interventions. *J Clin Med.* 2020;9(2):462.
8. Carcione JM, Santos JE, Bagaini C, Ba J. A simulation of a COVID-19 epidemic based on a deterministic SEIR model. *Front Public Health.* 2020;8:230.
9. Fang Y, Nie Y, Penny M. Transmission dynamics of the COVID-19 outbreak and effectiveness of government interventions: a data-driven analysis. *J Med Virol.* 2020;92(6):645-659.
10. Gao C, Tang S, Li W, Yang Y, Zheng Z. Dynamical processes and epidemic threshold on nonlinear coupled multiplex networks. *Physica A.* 2018;496:330-338.
11. Kabir KMA, Tanimoto J. Vaccination strategies in a two-layer SIR/V-UA epidemic model with costly information and buzz effect. *Commun Nonlinear Sci.* 2019;76:92-108.
12. Wang Z, Guo Q, Sun S, Xia C. The impact of awareness diffusion on SIR-like epidemics in multiplex networks. *Appl Math Comput.* 2019; 349:134-147.
13. Samanta S, Rana S, Sharma A, Misra AK, Chattopadhyay J. Effect of awareness programs by media on the epidemic outbreaks: S mathematical model. *Appl Math Comput.* 2013;219(12):6965-6977.
14. Fan C, Jin Y, Huo L, Liu C, Yang Y, Wang Y. Effect of individual behavior on the interplay between awareness and disease spreading in multiplex networks. *Physica A.* 2016;461:523-530.
15. Kan JQ, Zhang HF. Effects of awareness diffusion and self-initiated awareness behavior on epidemic spreading-an approach based on multiplex networks. *Commun Nonlinear Sci.* 2017;44:193-203.
16. Yang Z, Zeng Z, Wang K, et al. Modified SEIR and AI prediction of the epidemics trend of COVID-19 in China under public health interventions. *J Thorac Dis.* 2020;12(3):165-174.
17. Zhao S, Chen H. Modeling the epidemic dynamics and control of COVID-19 outbreak in China. *Quant Biol.* 2020;8(1):1-9.
18. Lei S, Jiang F, Su W, et al. Clinical characteristics and outcomes of patients undergoing surgeries during the incubation period of COVID-19 infection. *EClinicalMedicine.* 2020;21:100331.
19. Lauer SA, Grantz KH, Bi Q, et al. The incubation period of coronavirus disease 2019 (COVID-19) from publicly reported confirmed cases: estimation and application. *Ann Intern Med.* 2020; 172(9):577-582.
20. Kermack WO, McKendrick AG. A contribution to the mathematical theory of epidemics. *Proc R Soc London (Ser A).* 1927;115(772): 700-721.
21. Capasso V, Serio G. A generalization of the Kermack-McKendrick deterministic epidemic model. *Math Biosci.* 1978;42(1-2):43-61.
22. Inaba H. Kermack and McKendrick revisited: the variable susceptibility model for infectious diseases. *Jpn J Ind Appl Math.* 2001;18(2):273-292.
23. Liu X, Yang L. Stability analysis of an SEIQV epidemic model with saturated incidence rate. *Nonlinear Anal: Real World Appl.* 2012; 13(6):2671-2679.
24. Bai Y, Mu X. Global asymptotic stability of a generalized SIRS epidemic model with transfer from infectious to susceptible. *J Appl Anal Comput.* 2018;8(2):402-412.
25. DeJesus EX, Kaufman C. Routh-Hurwitz criterion in the examination of eigenvalues of a system of nonlinear ordinary differential equations. *Phys Rev A.* 1987;35(12):5288-5290.
26. Gil JJ, Avello A, Rubio A, Florez J. Stability analysis of a 1 DOF haptic interface using the Routh-Hurwitz criterion. *IEEE Trans Control Syst Technol.* 2004;12(4):583-588.
27. Hukushima K, Nemoto K. Exchange Monte Carlo method and application to spin glass simulations. *J Phys Soc Jpn.* 1996;65(6):1604-1608.
28. Lyubartsev AP, Martynovskii AA, Shevkunov SV, Vorontsov-Velyaminov PN. New approach to Monte Carlo calculation of the free energy: method of expanded ensembles. *J Chem Phys.* 1992; 96(3):1776-1783.
29. Xia S, Liu J. A belief-based model for characterizing the spread of awareness and its impacts on individuals' vaccination decisions. *J R Soc Interface.* 2014;11(94):20140013.
30. Chen YC, Lu PE, Chang CS, Liu TH. A time-dependent SIR model for COVID-19 with undetectable infected persons. *IEEE Trans Netw Sci Eng.* 2020;7(4):3279-3294.

**How to cite this article:** Zhao X, Zhou Q, Wang A, Zhu F, Meng Z, Zuo C. The impact of awareness diffusion on the spread of COVID-19 based on a two-layer SEIR/V-UA epidemic model. *J Med Virol.* 2021;93:4342-4350.  
<https://doi.org/10.1002/jmv.26945>